A Fresh Look for Natural Fracture Characterization Using Advance Borehole Acoustics Techniques*

Willem Veltman[1], Edgar Velez[2], and Violeta Lujan[2]

Search and Discovery Article #40915 (2012)
Posted April 16, 2012

*Adapted from extended abstract prepared in conjunction with oral presentation at AAPG Annual Convention and Exhibition, Long Beach, California, April 22-25, 2012, AAPG©2012

[1]GPA Energy, Saltillo Area, Mexico
[2]Schlumberger, Ltd., Mexico (earteaga3@slb.com)

Abstract

A new workflow reliably characterizes natural fractures in the complex Sabinas Basin in northern Mexico, where image logs alone have been unable to characterize fracture networks adequately. The new approach, which integrates the response of borehole images with advanced dipole sonic tool measurements, directly impacts the decision criteria of producible intervals where the zones that produce are the zones with open fractures that may be seen not only in the borehole image but also in the acoustic anisotropy and Stoneley attenuation. A case study of two wells in the Sabinas Basin shows how the methodology gives a quantitative way to better understand the fracture networks and fracture dynamics in naturally fractured reservoirs, establishing a novel criterion for fast decisions based on colored flags.

Introduction

The Sabinas Basin is located in northeastern Mexico in the states of Coahuila and Nuevo Leon (Figure 1). The basin of 37,000 square kilometers contains more than 5000 meters of sediments, corresponding to the Late Jurassic Series (Oxfordian through Tithoninan). This formation consists of irregular, alternating layers of highly bituminous and carbonaceous limestone, sandstone, shale, and conglomerate. Drilling depths generally vary around 1800 to 4500 meters. The Sabinas Basin contains rocks ranging from Triassic through the Paleocene that underwent deformation during the Tertiary and are highly faulted. The stratigraphic evolution is complex, encompassing three super cycles with complex cyclical sedimentation. The reservoir rocks have low porosity and low permeability and mainly produce from fractures.

The operators in the basin have been acquiring standard logs and borehole images for fracture identification. They have identified conductive, partial, and induced fractures, but production logs show that only a few of the identified fractures have actually been open fractures. These open fractures make the difference in this field because they enable the operator to estimate reserves.

The production of these fields has been associated with fractures, and for that reason the logging suite includes acoustic and borehole image logs to quantitatively evaluate the impact of the fractures on well productivity and completion design. We implemented a workflow integrating the response of borehole images and the acoustic scanning platform together with the basic log information. The integration involves fracture identification of the borehole images, Stoneley processing, and anisotropy with dispersion analysis from the acoustic scanning platform. The anisotropy results and the fractures identified with the borehole images are then integrated with a forward-modeling approach. The results of these responses are compared with additional information such as production logs, mud logging events, or reservoir samples to finally characterize producible fractures. Identifying and characterizing fractures are fundamental activities during the life cycle of a naturally fractured reservoir. These activities can make the difference between drilling a nonproducing well and a producing well, and the workflow described here provides a good understanding of fracture networks and fracture dynamic properties.

Background - Regional Context

The Sabinas Basin is in a depression formed by a series of subsided blocks that elevates to the northwest and separates the Sabinas Basin from the Chihuahua Basin. High blocks of smaller dimension exist in the depression (Monclova highs and la Mula). Meanwhile, toward the southeast, other blocks formed the boundary separating the Sabinas Basin from the proto Gulf of Mexico, and communication with the Central Mexican Basin was established through a trough of low blocks situated between the high blocks of Miquihuana and Coahuila. Toward the basin margins where Jurassic evaporates are absent, faults are emergent, and very high relief anticline structures occur.

Fracture systems are well developed in the structures of the Sabinas Basin. According to Nelson's (1985) classification, these are of Type 1(ab) and Type 2 (ac), forming suborthogonal grids that can be observed in outcrops, conventional cores, aerial photographs, and satellite images. Fracture density is greater in compacted, coarse-grained siliciclastic rocks and dolomites than in limestone and siliciclastic mudstones. Compacted limestone could be a good seal for hydrocarbons because its degree of fracturing is minimal. Although gas reservoirs in the basin are generally found in the structures above basement highs near antithetic faults, they also appear in other formations, in which brittle folded strata and fracture systems develop. Finally, the geomechanics borehole breakout analysis of this basin indicates that the present regional minimal stress component SHmin is an active extension, trending north to northwest/southeast, possibly resulting from compression (SHmax) perpendicular to the present continental margin.

The production history of the basin dates from 1979, when the basin peaked at 160 MMcf/D. Between 1984 and 1991 production in the Monclova-Buena Suerte and Lampazos fields stabilized at 11 MMcf/D; with the development of the Merced Field in 1995, production increased to about 60 MMcf/D, but decreased to 18 MMcf/D by 2000 when the development of the fields in the basin almost stopped. At the end of 2003 and beginning of 2004, a new development campaign started with two exploration wells operated by the Mexican national oil company, Pemex.

Fracture Productivity and Horizontal Stress Orientation

Because this basin is a gas producer in a naturally fractured reservoir, fracture identification is not the only important consideration; fracture direction and their relationship with the principal stresses is valuable in determining the critically stressed fractures that are the most suitable to produce and sustain production longer. In all the wells evaluated in this basin, the open fractures aligned with the maximum horizontal stress direction are the main contributors to well production.

Fracture Identification in Boreholes Using Microelectrical Images

Borehole images from microelectrical tools have become essential sources of identification potential in gas reservoirs. One of the benefits of these images is their vertical resolution (5 mm) that, with almost fullbore coverage in standard diameter boreholes, can assure that no features are missed along the borehole wall. Generally, the interpretation of borehole images includes bedding and structural as well as textural and fracture characterization.

The identification of fractures is based on the observation of a resistivity contrast with the host rock for electric tools (classified as conductive or resistive fractures). Conductive fractures are generally considered to be open, but they also may be clay-filled (a rare case, although they may be filled with another conductive mineral). Resistive fractures are preferentially filled with resistive minerals such as calcite and quartz (Figure 2).

From the image morphology, different fracture types can be identified and classified into natural fractures and stress-induced fractures. Stress-induced fractures result from the combination of far-field, unequal principal stresses, near-field stress concentrations around the borehole, and stress perturbation during drilling operations (mud pressure and thermal effects). Two sets of principal stresses are important in the analysis of wellbore rock mechanics, far-field stresses and wellbore stresses (Krabbe et al., 1999). Far-field stresses are not influenced by the borehole because they exist in the formation far away from the wellbore. In contrast, wellbore stresses act on the formation at the mud/formation interface, and they are controlled by the mud density as well as the far-field stresses. Stress-induced fractures are generally classified using the mode of origin, shear and tensile failure modes, and the morphology (wide or narrow breakout, high-angle echelon, etc., Krabbe et al., 1999).

The determination of the geometrical properties of the fractures includes the location and orientation of the ideal-plane representation of the fractures (given as depth, dip angle, and dip azimuth). Fracture apertures can also be measured from image logs (Luthi and Souhaite, 1990), and are typically on the order of 10 μm to 2 mm. Another important parameter for the evaluation of fractures is the average fracture intensity, defined as the number of fractures over a distance in the direction orthogonal to fracture planes (average fracture spacing is the inverse of fracture intensity).

Anisotropy and Sonic Waveform Dispersion Analysis

Shear waves propagate through rocks with different velocities in different directions. This phenomenon is called *acoustic anisotropy,* and it is caused by the anisotropic nature of the rock's elastic properties. All sedimentary rocks exhibit some degree of acoustic anisotropy related to aligned fractures, layering, or stress imbalance. From the azimuthal anisotropy analysis of cross-dipole waveforms, fast-shear azimuths are calculated using a method such as Alford rotation (Boyd et al., 1994).

To identify the rock anisotropy mechanism, we use a technique called dispersion analysis (Plona et al., 2000). From this analysis we can divide the formation into four cases (Figure 3):

1) Homogenous isotropic - in this case no shear wave splitting occurs, this is a very stable situation where the dipole dispersion from the field data and the one theoretically computed from the homogeneous isotropic (HI) model overlay.

2) Heterogeneous isotropic - in this case no shear wave splitting occurs but the dipole dispersion from field data is steeper than the HI model dispersion.

3) Homogenous anisotropic - in this case shear wave splitting exist and the fast (red curve) and slow (blue curve) slowness are different across all the frequency range, this anisotropy is associated with intrinsic anisotropy such as layering or fractures.

4) Heterogeneous anisotropic - in this case shear wave splitting exist but velocities are crossing over across the frequency range, where the slow shear slowness becomes faster than the fast shear slowness towards near well bore area (high frequency). This is a result of differential interaction between hoop stress and far field stresses and is associated to stress induced anisotropy.

Stoneley Reflection and Transmission Analysis

Stoneley attenuation and reflection coefficients indicate open fractures. When Stoneley waves propagate through an open fracture, some of the energy is reflected and some is transmitted. Stoneley attenuation is evaluated with the normalized difference energies (NDE) techniques (Brie et al., 1998). The objective of the technique is to correlate the attenuation and reflection coefficients together with the variable density log (VDL) chevron patterns from the Stoneley acquisition mode with the borehole image information.

Fracture Anisotropy Modeling

Fracture anisotropy modeling is a methodology that integrates the response of the fractures (natural and induced) from the borehole image and compares it with the response of the anisotropy response of the acoustic scanning platform log that probes the formation at different depths of investigation around the borehole. Fracture anisotropy modeling uses a forward-modeling approach that combines a classical excess compliance fracture model that relies on the orientation of the individual fractures, the elastic properties of the host rock, and the normal and tangential fracture-compliance parameters (Prioul et al., 2007). When several planar fractures of various orientations are present and identified on image logs, they increase the effective elastic compliance of the medium and consequently increase the wave slowness (that is, they decrease the wave velocities). When the average fracture spacing is much smaller than the wavelength, effective-medium models can be applied (Prioul et al., 2007).

The results of the fracture anisotropy modeling allow classifying the formation into three types:

1) fracture induced
2) stress induced
3) mixed mechanism (stress and fractures)
4) unknown

Applied Workflow

Most workflows for fracture characterization tend to compare in a qualitative way the strike direction of the fractures (natural and induced) from the borehole images with the direction of the azimuth of the fast shear, aiming to identify the zones of lateral continuity of these events. That this could lead to some unknowns where azimuthal projections of the fast shear depend on the reference plane used (north, borehole, and earth).

The main objective of our workflow (Figure 4) is to integrate all the information available for fracture characterization, including the basic standard logs, calipers, and Stoneley reflection and transmission analysis, complementing this information with the quantitative integration of the borehole images and the anisotropy response from the acoustic scanning platform using the fracture anisotropy modeling methodology. Finally, we correlate the information with reservoir dynamic information like formation testing samples, mud logging kickoffs, and production logging results to identify the fractures and directions of those that contribute more in terms of production. Once the more producible fractures and their directions are identified, the information can be used to determine the preferred drilling direction (perpendicular to producible fractures) or to select producible intervals in cases where casing and cement are needed.

Case Study Results

Case 1

The typical open and induced fracture orientation image processing of this field is reflected in Figure 5. When the sonic direction observed is related to the same orientation for both open and induced fractures, these are the best wells of the field.

In the first case of study, mineralogy was obtained from standard logs that indicated a combination of quartz, calcite, and illite. This reservoir is highly fractured and it needs a combination of borehole images and advanced sonic processing. From borehole imaging in this case, we identified several fractures along the logged interval, which we classified as conductive, resistive, and induced. One preferential direction detected for the open fractures was NW 360.

However, before we used the workflow anisotropy modeling (Figure 6) to specify the locations of the open fractures, we knew that the more productive fractures were the ones that were aligned with the maximum horizontal stress direction, so we needed to look at the fracture anisotropy modeling, which identified the zones with the black flags (stress driven) or green flags (fracture driven) aligned in the direction of the maximum horizontal stress. Applying the criteria above, we selected the fractures with the best potential to produce in the entire interval. From Figure 6 we can interpret that this reservoir is highly fractured, and most of the fractures appear to be open in both the image and acoustic logs, so the reflections of the Stoneley waves are very much in tune with the results of the workflow that we propose.

For this case study the results were compared with the mud log (Figure 7), which appears at Track 10. In this track we can associate the flags of open fractures with the result of gas kicks in the mud log, which really correlates with the combined method proposed as a workflow.

Case 2

In the second case study, we acquired the same logging information. In this case the mineralogy differs from the previous case; we have more calcite and less quartz material. As described previously, we know that this reservoir produces from fractures, which is why the mineralogy was not the main factor of the workflow. In this figure the interpretation of the borehole image maintained the same pattern as the previous case, with open conductive fractures, resistive fractures, and induced fractures. After using the anisotropy modeling, we could differentiate the open fractures from the closed ones.

Stoneley reflections seem more active at the zone of x600 to x670 m, and it is associated with the fractures observed on the borehole images, adding to this all the anisotropy indicators, time, slowness, and increments of maximum energy, the model agrees with the interval and the fracture were classified as open fractures.

Finally, for this case of study (Figure 9), using the fracture discrimination with the new workflow led to a good match between the mud log and our results; however, in this case we used the radial profiles of the advanced sonic processing plus the interpretation of borehole processing, which confirmed again that the zone of interest is at x660 to x700 m.

Conclusions

In this paper we have presented a comprehensive workflow, used in a northern Mexico region, that has proven to be a robust solution for fracture characterization and fracture dynamic properties in naturally fractured reservoirs. This workflow combines the classical information from standard logs and oriented caliper analysis with the Stoneley analysis and fracture anisotropy modeling for a quantitative understanding of borehole image information and its acoustic anisotropy response.

For these case studies in the Sabinas Basin, we have now established new criteria to identify potential producible zones that will allow making fast decisions based on colored flags and the maximum horizontal stress direction. These criteria can easily be optimized per field with the combination of mud logs or production logs.

References

Brie, K., C. Eckersley, and K. Hsu, 1988, Using the Stoneley normalized differential energies for fractured reservoir evaluation: 29th SPWLA Logging Symposium, 25 p.

Boyd, A., S. Denoo, C. Esmersoy, and M. Kane, 1995, Fracture and stress evaluation using dipole-shear anisotropy logs: 36th SPWLA Annual Logging Symposium, 10 p.

Krabbe, H., D. Plumb, J. Rasmus, Q. Li, T. Bornemann, and T. Bratton, 1999, Logging-while-drilling images for geomechanical, geological and petrophysical interpretations: 40th Annual SPWLA Logging Symposium, Expanded Abstracts, p. 1-14.

Luthi, S.M., and P. Souhaite, 1990, Fracture apertures from electrical borehole scans: Geophysics, v. 55/7, p. 821-833.

Nelson, R.A., 1985, Geologic analysis of naturally fractured reservoirs: Gulf Publishing Company.

Plona, T.J., B.K. Sinha, M.R. Kane, and O. Viloria, 2000, Using acoustic anisotropy: 41st SPWLA Annual Logging Symposium, 12 p.

Prioul, R., D. Adam, R. Koepsell, Z. El Marzouki, and T. Bratton, 2007, Forward modeling of fracture-induced sonic aisotropy using a combination of borehole image and sonic logs: Geophysics, v. 72/4, p. 135-147.

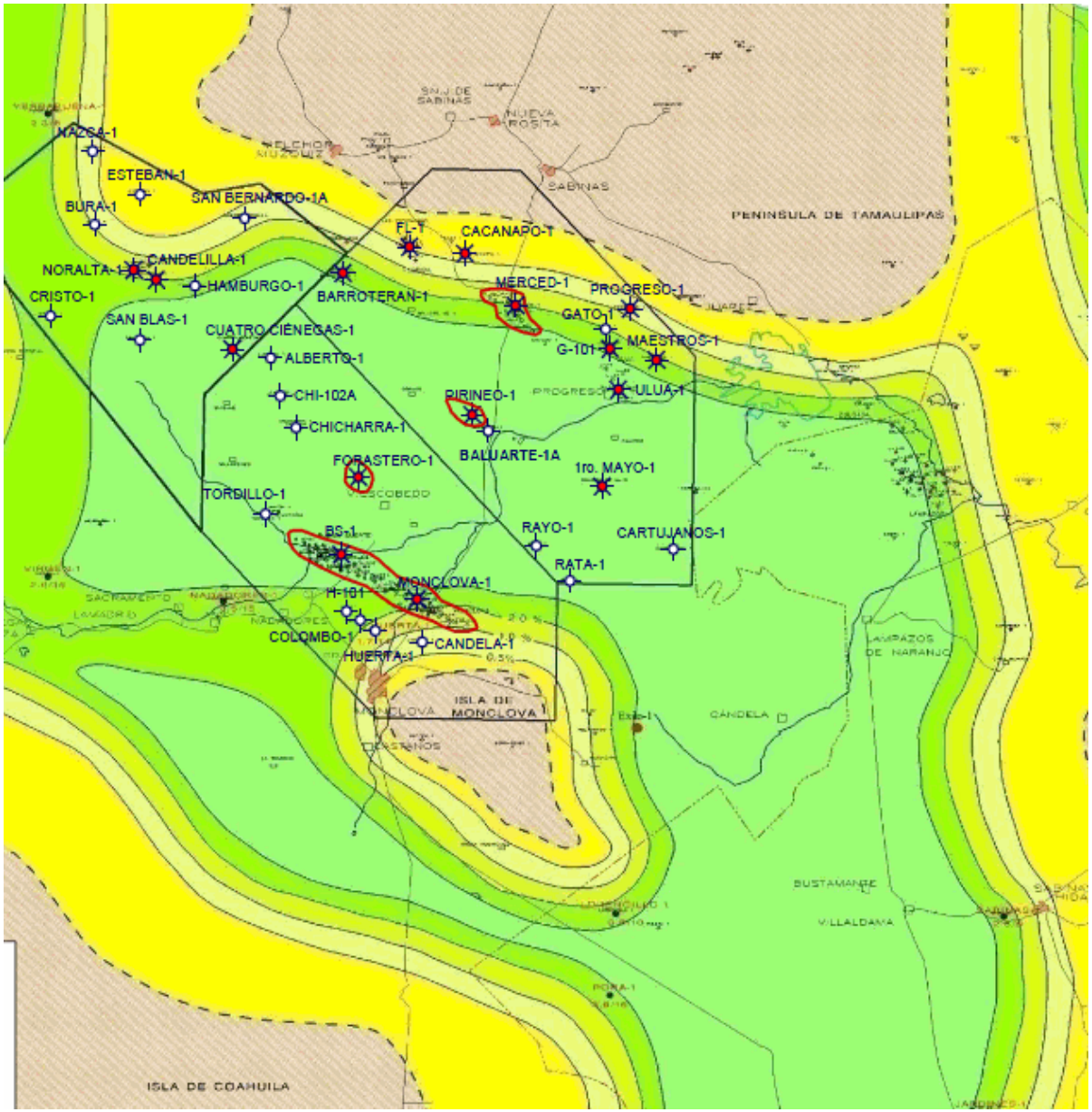

Figure 1. Sabinas Basin located in northern Mexico.

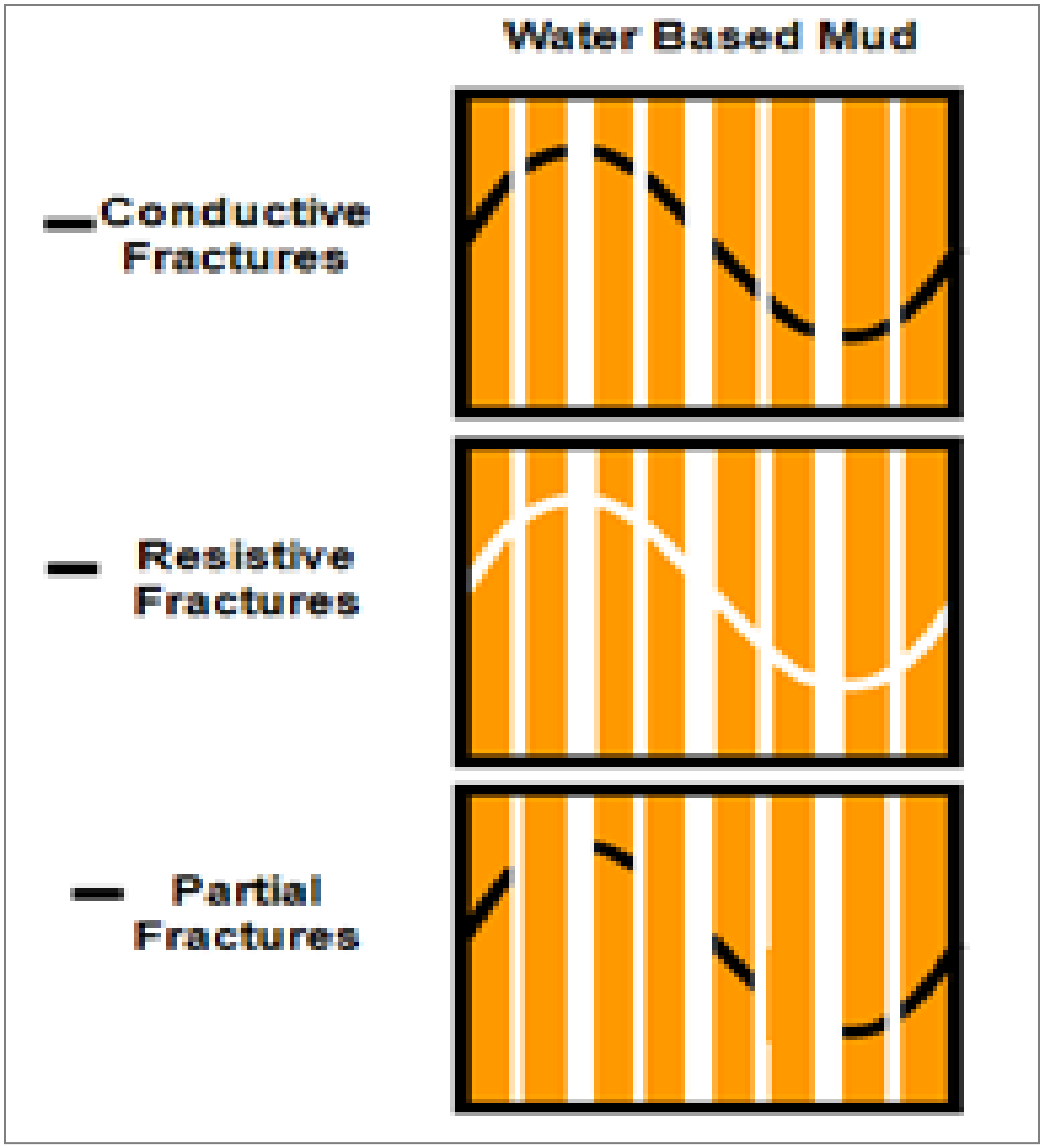

Figure 2. Fracture characteristics depend on resistivity contrast in water-based mud.

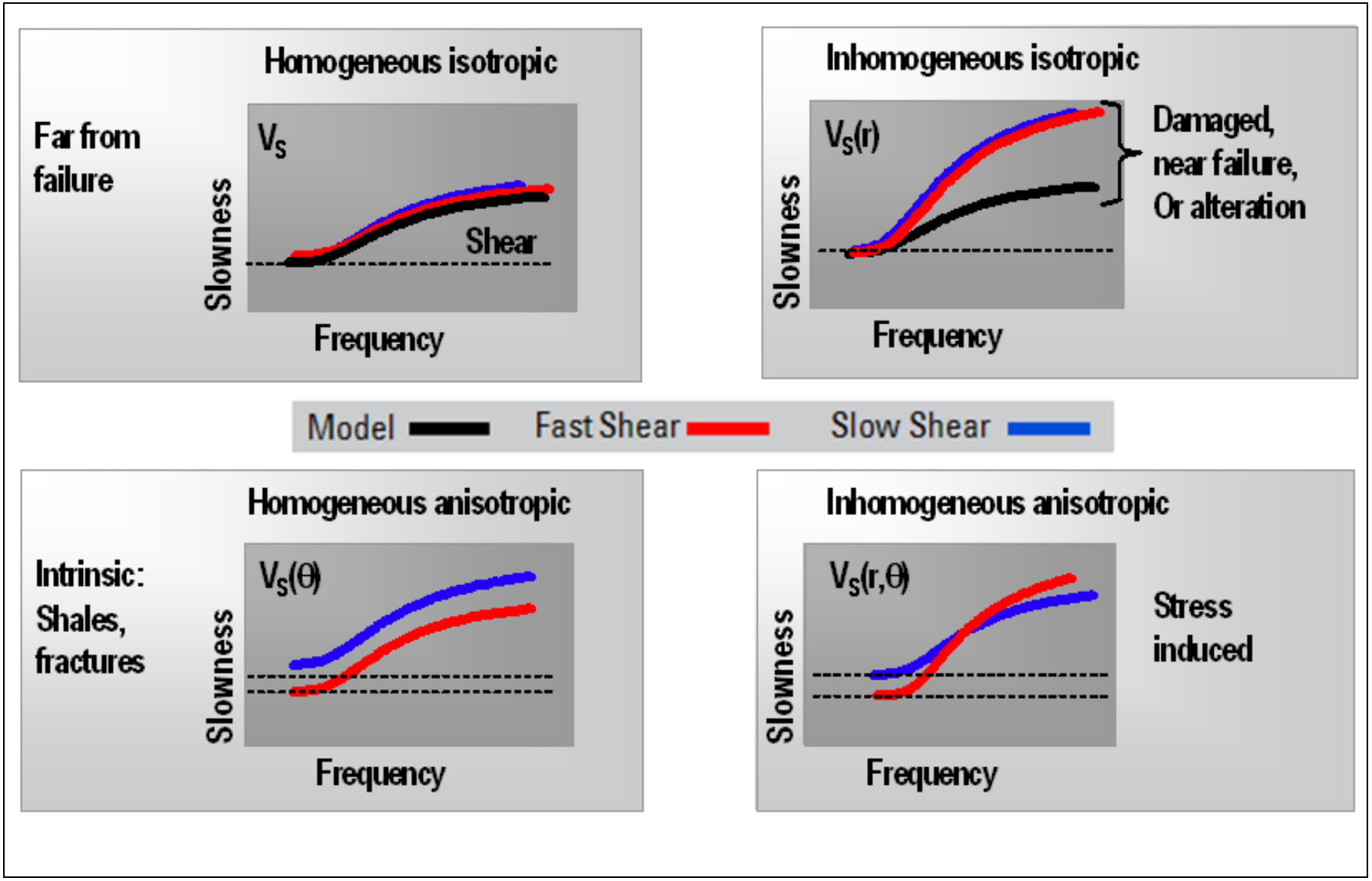

Figure 3. Dispersion analysis for fracture anisotropy characterization: a) homogeneous isotropic, b) heterogeneous isotropic, c) homogenous anisotropic, d) heterogeneous anisotropic.

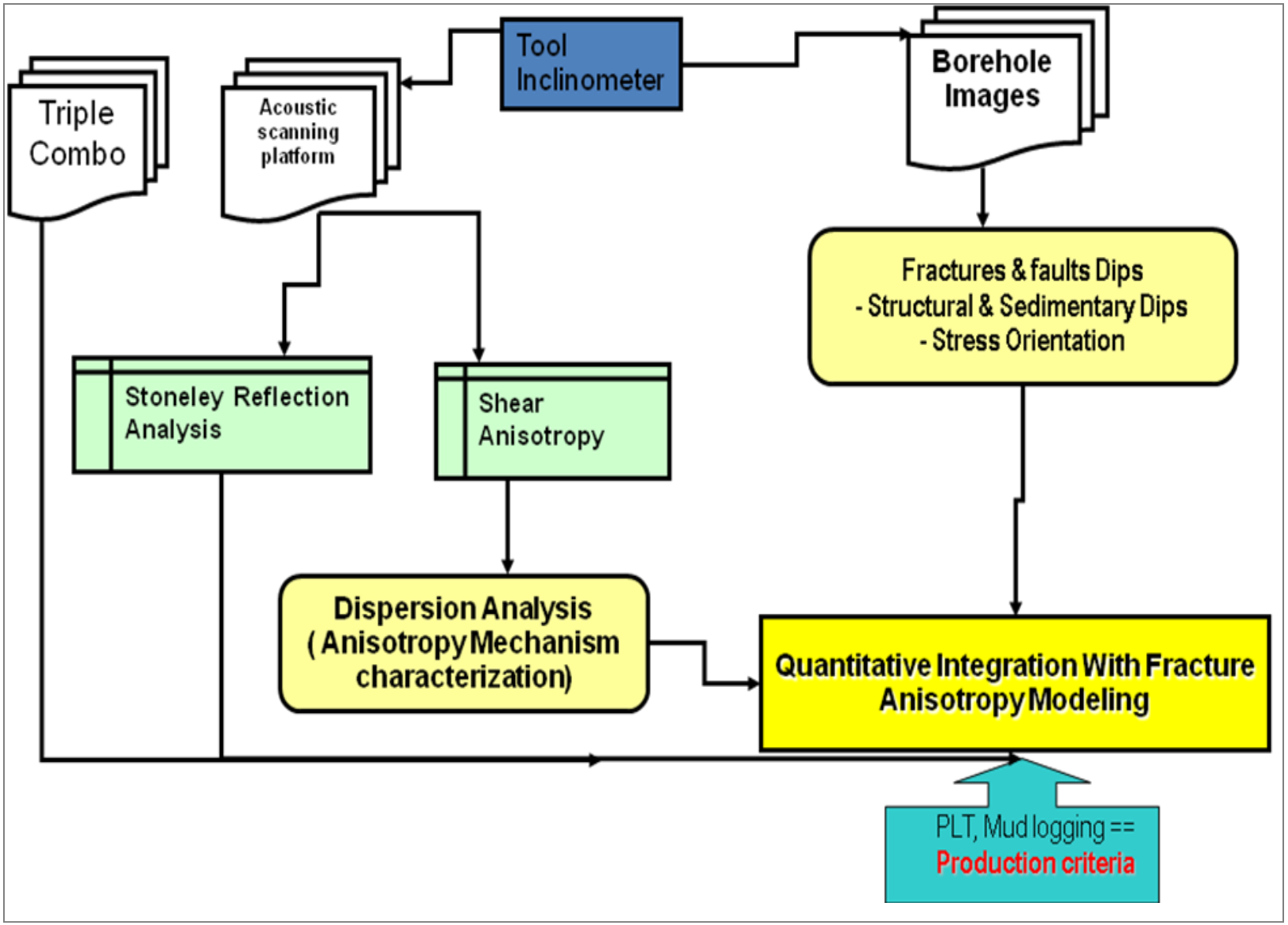

Figure 4. Workflow combines fracture characterization information with borehole images and anisotropy responses to improve modeling.

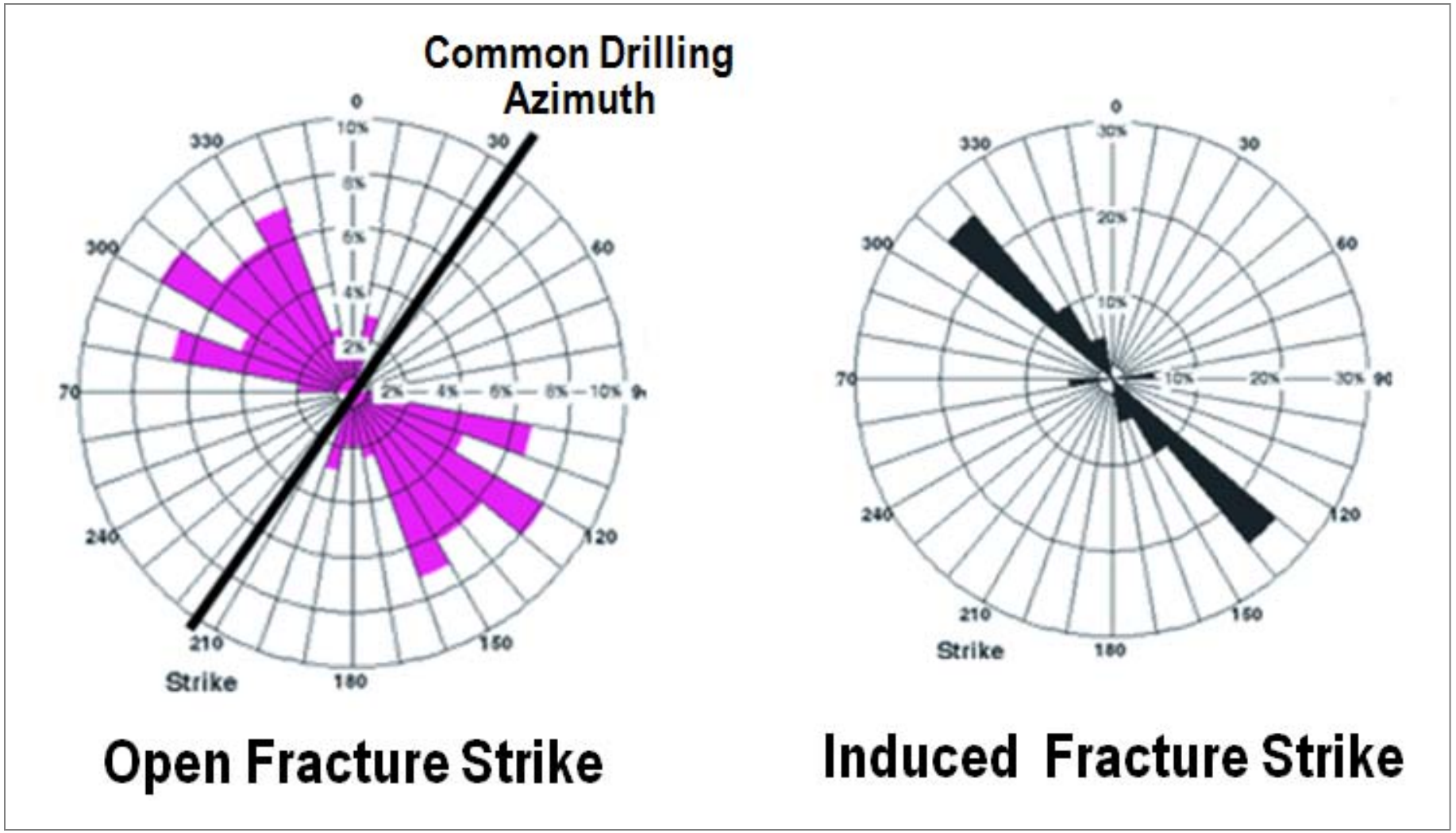

Figure 5. Open fracture orientation using borehole processing and advanced sonic processing.

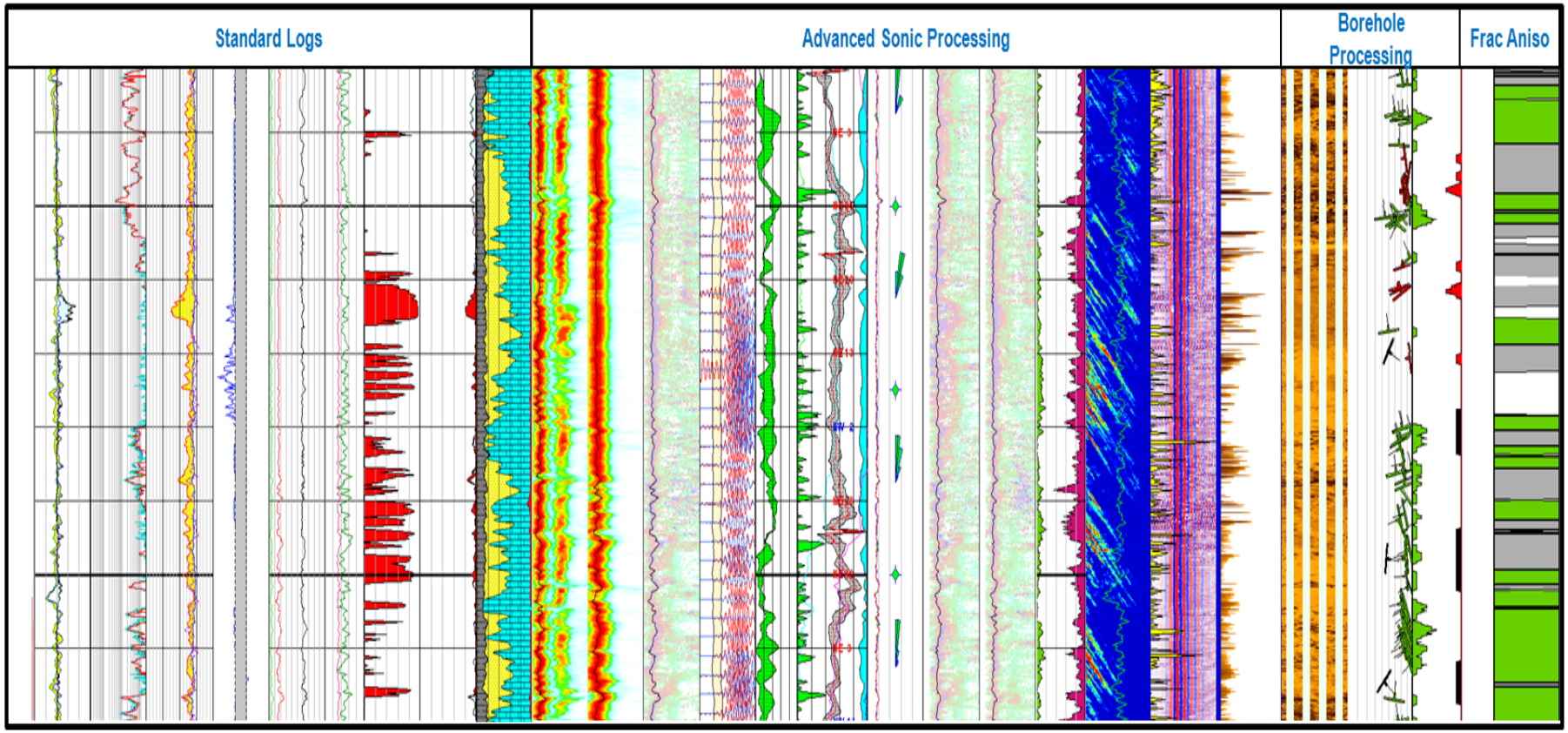

Figure 6. Anisotropy modeling shows that the reservoir is highly fractured; the new model matches well with Stoneley waves.

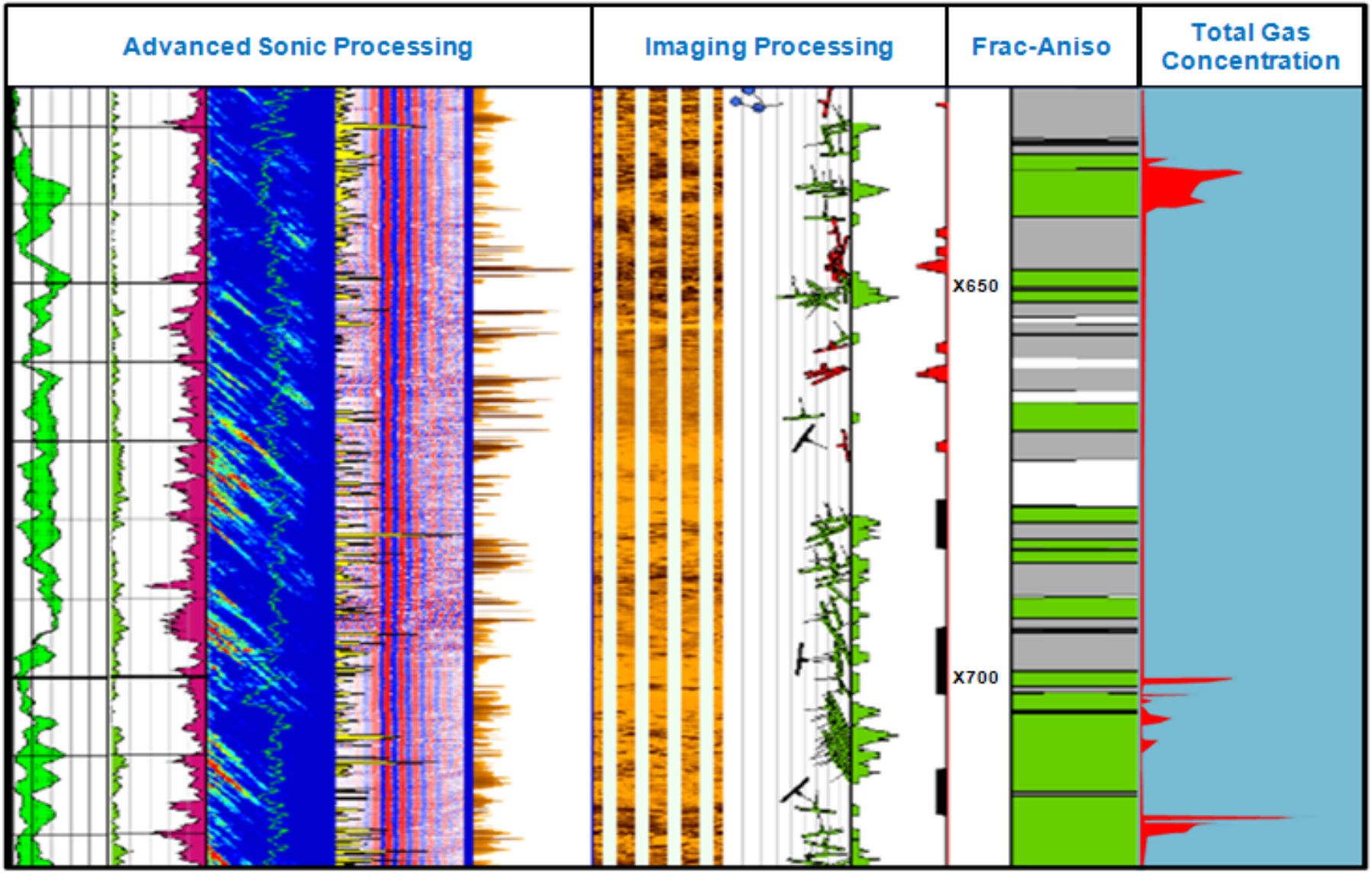

Figure 7. Using the combined method and mud logs to select the best intervals.

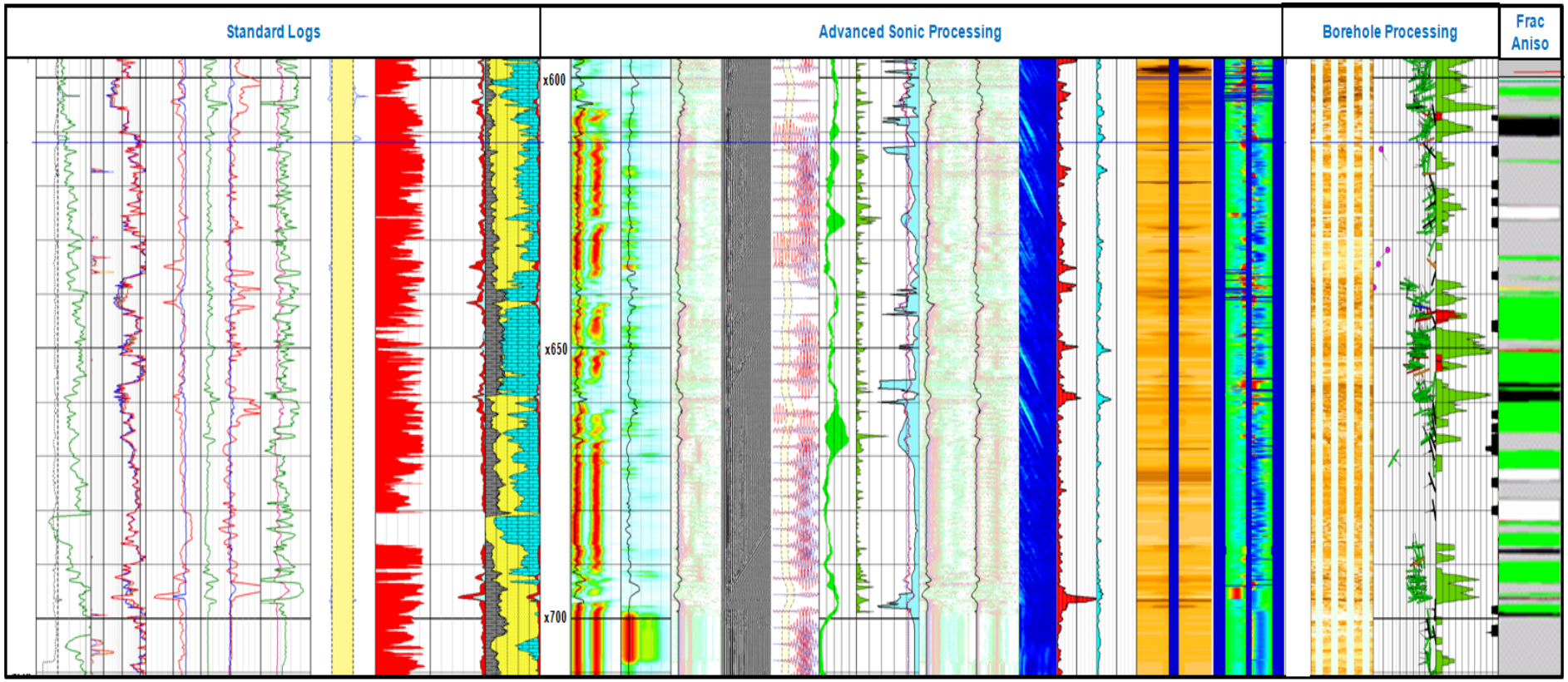

Figure 8. Results of the combination of measurements in the second case study.

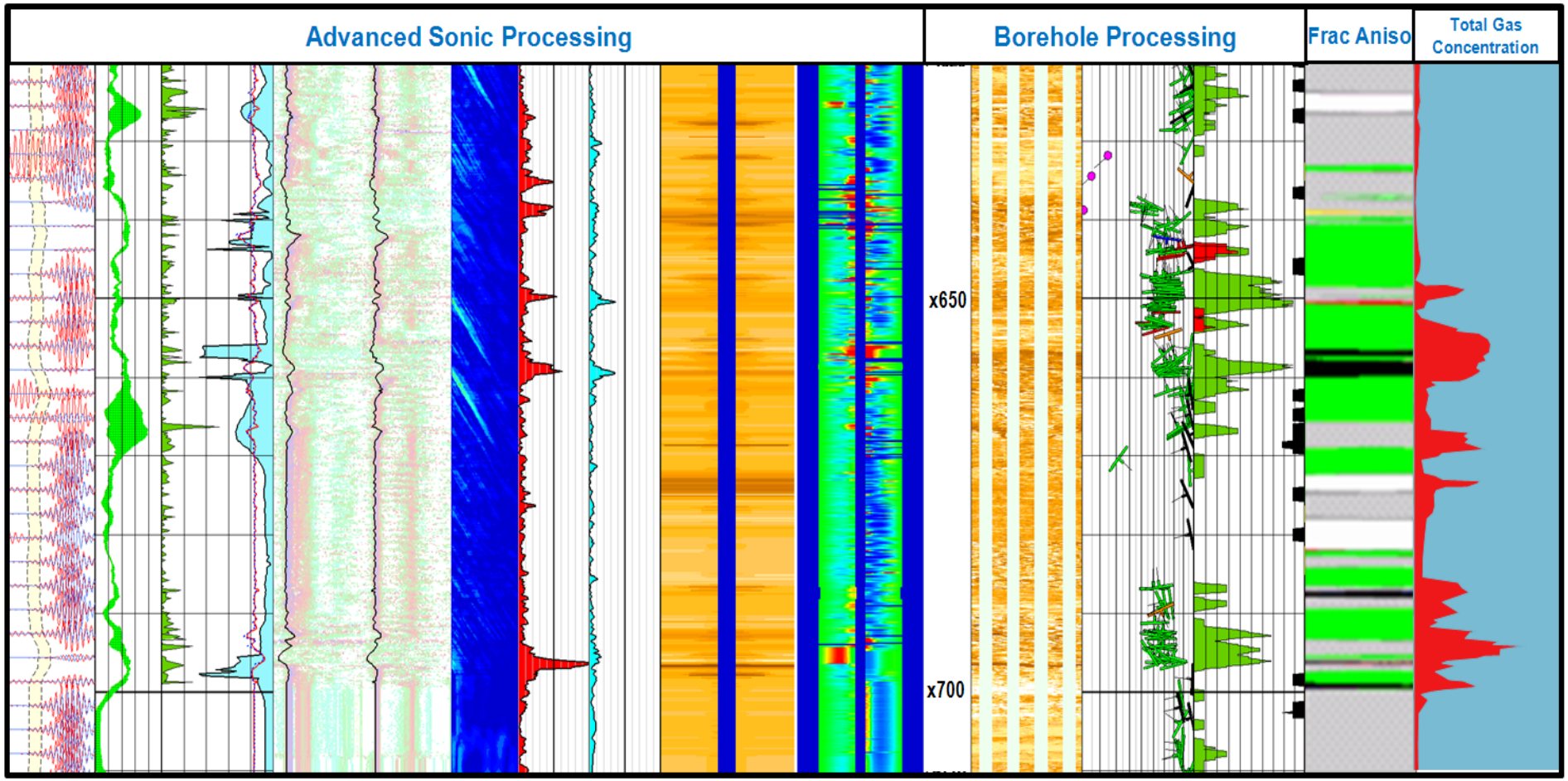

Figure 9. Using the combined method and mud logs and advanced sonic processing.